Biochimica et Biophysica Acta 1853 (2015) 1060–1072

Contents lists available at ScienceDirect

Biochimica et Biophysica Acta

journal homepage: www.elsevier.com/locate/bbamcr

YAF2 promotes TP53-mediated genotoxic stress response via stabilization of PDCD5

Soo-Yeon Park [a,1], Hyo-Kyoung Choi [a,1], Seong-Ho Jo [a], JaeSung Seo [a], Eun-Jeong Han [a], Kyung-Chul Choi [b], Jae-Wook Jeong [c], Youngsok Choi [d,*], Ho-Geun Yoon [a,*]

[a] Department of Biochemistry and Molecular Biology, Brain Korea 21 PLUS Project for Medical Sciences, Yonsei University College of Medicine, Seoul, Republic of Korea
[b] Department of Biomedical Sciences, University of Ulsan College of Medicine, Seoul, Republic of Korea
[c] Department of Obstetrics, Gynecology & Reproductive Biology, Michigan State University College of Human Medicine, MI, USA
[d] Fertility Center of CHA General Hospital, CHA Research Institute, CHA University, Seoul, Republic of Korea

ARTICLE INFO

Article history:
Received 5 December 2014
Received in revised form 7 January 2015
Accepted 9 January 2015
Available online 17 January 2015

Keywords:
Genotoxic stress
PDCD5
YAF2
TP53
Apoptosis

ABSTRACT

Programmed cell death 5 (PDCD5) plays a crucial role in TP53-mediated apoptosis, but the regulatory mechanism of PDCD5 itself during apoptosis remains obscure. We identified YY1-associated factor 2 (YAF2) as a novel PDCD5-interacting protein in a yeast two-hybrid screen for PDCD5-interacting proteins. We found that YY1-associated factor 2 (YAF2) binds to and increases PDCD5 stability by inhibiting the ubiquitin-dependent proteosomal degradation pathway. However, knocking-down of YAF2 diminishes the levels of PDCD5 protein but not the levels of PDCD5 mRNA. Upon genotoxic stress response, YAF2 promotes TP53 activation via association with PDCD5. Strikingly, YAF2 failed to promote TP53 activation in the deletion of PDCD5, whereas restoration of wild-type $PDCD5^{WT}$ efficiently reversed the ineffectiveness of YAF2 on TP53 activation. Conversely, PDCD5 efficiently overcame the knockdown effect of YAF2 on ET-induced TP53 activation. Finally, impaired apoptosis upon PDCD5 ablation was substantially rescued by restoration of $PDCD5^{WT}$ but not YAF2-interacting defective $PDCD5^{E4D}$ nor TP53-interacting defective $PDCD5^{E16D}$ mutant. Our findings uncovered an apoptotic signaling cascade linking YAF2, PDCD5, and TP53 during genotoxic stress responses.

1. Introduction

Tumor suppressor TP53 is a critical transcriptional factor and plays a central role in the regulation of cell cycle, DNA repair, apoptosis, senescence, and angiogenesis [1]. The function of TP53 is tightly controlled by its binding partners and post-translational modifications [2,3]. Under normal conditions, TP53 is maintained at a low level by interacting with E3 ubiquitin ligases such as MDM2, Pirh2, COP1, and ARF-BP1, which mediate TP53 degradation by the ubiquitin–proteasome pathway [4–7]. In contrast, under stress conditions, TP53 is stabilized by factors such as p300, ATM, and HIPK2 and is activated to function as a transcription activator and regulator of downstream target genes for cell cycle arrest and apoptosis [8–10]. Although much research has uncovered an impressive number of TP53-interacting proteins, MDM2 and MDMX proteins are most highlighted as promising targets of cancer therapy [11]. Most small molecules that directly or indirectly activate the TP53 response are TP53-MDM2 interaction inhibitors [12]. Although MDM2 inhibitors are shown to effectively reactivate TP53 in vivo, there are still limited applications for retaining mutant TP53 or deleted TP53 [13,14]. Thus, further understanding of the TP53 network could lead to the development of selective and potent chemotherapy.

Programmed cell death 5 (PDCD5), formerly designated TFAR19 (TF-1 cell apoptosis related gene-19), is a novel gene from TF-1 cells undergoing cytokine deprivation-induced apoptosis. The gene is widely expressed in a variety of tissues, although its mRNA expression in fetal tissue is significantly lower than in adult tissue [15]. Recent findings demonstrated the role of PDCD5 in the immunoregulation and its mRNA levels and protein expression are significantly decreased in psoriasis [16,17]. When overexpressed in cancer cell lines, PDCD5 facilitates apoptosis triggered by certain stimuli and enhances TAJ/TROY-induced paraptosis-like cell death. When cells are undergoing apoptosis, PDCD5 expression is rapidly upregulated, and the protein is translocated from the cytoplasm to the nucleus [18]. Restoration of PDCD5 with recombinant protein or an adenovirus expression vector can significantly sensitize different cancers to chemotherapies [19,20]. In addition, single-nucleotide polymorphisms in the PDCD5 regulatory region are

Abbreviations: PDCD5, Programmed cell death 5; YAF2, YY1-associated factor 2; ET, etoposide

* Corresponding authors at: Department of Biochemistry and Molecular Biology, Yonsei University College of Medicine, Seoul 120-752, Republic of Korea. Fax: +82 2 312 5041.
E-mail addresses: youngsokchoi@cha.ac.kr (Y. Choi), yhgeun@yuhs.ac (H.-G. Yoon).

[1] S.Y.P and H.K.C. contributed equally to this work.

http://dx.doi.org/10.1016/j.bbamcr.2015.01.006
0167-4889/

associated with chronic myelogenous leukemia and lung cancer [21,22]. Decreased PDCD5 expression has been reported in various human tumors, such as breast cancer [23], hepatocellular carcinoma [24], lung cancer [22], gastric cancer [25], astrocytic glioma [26], chondrosarcoma, and ovarian carcinoma [27]. These findings suggest decreased PDCD5 expression may be associated with carcinoma formation and malignant progression. Recent studies demonstrated that PDCD5 interacts with Tip60, enhances histone and TP53 K120 acetylation, and promotes BAX expression, consequently accelerating apoptosis after UV irradiation [28]. PDCD5 enhances TP53 stability by inhibiting MDM2-induced TP53 ubiquitination, nuclear export and proteasomal degradation [29]. Based on accumulated evidence, PDCD5 likely plays a positive regulatory role in the TP53 pathway. However, the molecular mechanism PDCD5's regulation during apoptosis remains unclear.

To understand the regulatory mechanism of tumor suppressor PDCD5 during apoptosis, we employed yeast two-hybrid assays to identify PDCD5's interacting partners and found that YAF2 binds to PDCD5 in response to genotoxic stress. We showed that YAF2 selectively increases the accumulation of PDCD5 protein by inhibiting ubiquitination of PDCD5. Moreover, knocking-down of YAF2 greatly diminishes PDCD5 stabilization as well as TP53 in response to etoposide (ET). We finally demonstrated that YAF2 promotes TP53-mediated genotoxic stress response in a PDCD5-dependent manner. Finally, we describe an apoptotic signaling cascade linking YAF2, PDCD5, and TP53 during genotoxic stress responses.

2. Materials and methods

2.1. Generation of *Pdcd5*$^{flox/flox}$ MEFs, cancer cell culture, and reagents

Human lung adenocarcinoma cell line A549, human colorectal carcinoma cell line HCT116 (TP53$^{+/+}$), and HCT116 (TP53$^{-/-}$) were purchased from and authenticated by the Korean Cell Line Bank (Seoul, South Korea) using short tandem repeat analysis. These cells were used within 6 months of purchases. All cells were cultured in Dulbecco's modified Eagle's medium (DMEM) supplemented with 10% (v/v) fetal bovine serum (FBS), 100 U/ml penicillin, and 0.1 mg/ml streptomycin (Hyclone, Logan, UT, USA) at 37 °C under 5% CO_2. Wild-type and *Pdcd5*$^{f/f}$ MEF cells were prepared as described previously [30]. These MEF cells were used for all subsequent experiments. MEF cells were maintained in DMEM containing 15% FBS (GIBCO BRL, Gaithersburg, MD, USA) and subcultured 1:3 upon reaching confluence. For electroporation of MEFs (3rd passage), 5 μg of plasmids was electroporated into a suspension of MEF cells (2×10^5 cells) using a Neon transfection system (Life Technologies, Grand Island, NY, USA). Etoposide (ET) and cycloheximide were purchased from Sigma-Aldrich (St. Louis, MO, USA), and MG-132 was purchased from Calbiochem (Darmstadt, Germany). Etoposide and MG-132 were prepared in dimethyl sulfoxide (DMSO) (Sigma-Aldrich). Nutlin3a is from Sigma-Aldrich. Tenovin-6 was purchased from Santa Cruz Biotechnology (Santa Cruz, CA, USA). Control cultures received the same amounts of DMSO, and final DMSO concentrations did not exceed 0.1%. Transient transfection was performed using Polyexpress (Excel Gene, Rockville, MD, USA).

2.2. Immunoprecipitation (IP) and antibodies

Antibodies against p53 (sc-126), p21, pro-PARP-1 and HA were purchased from Santa Cruz Biotechnology Inc. (Santa Cruz, CA, USA). Antibody against γH2AX was purchased from Epitomics (Burlingame, CA, USA). Antibody against PDCD5 was purchased from Proteintech Group Inc. (Chicago, IL, USA). FLAG and β-actin antibodies were obtained from Sigma-Aldrich. Myc, pro-caspase-3, cleaved-caspase-3 antibodies were purchased from Cell Signaling (Beverly, MA, USA). Cleaved-PARP-1 (51-6639GR) antibody was purchased from BD Transduction Laboratories (Lexington, KY, USA). Bax and Puma antibodies were purchased from Abcam (Cambridge, MA, USA). The antibody against YAF2 was generated by LabFrontier (Anyang, South Korea) using the synthetic peptide MGDKKSPTRPKRQPKPSS.

2.3. Yeast two-hybrid screening

The Matchmaker™ Gold Yeast Two-Hybrid System (Clontech Laboratories, Mountain View, CA, USA) was used for yeast two-hybrid screening according to the manufacture's protocol with minor modification. Briefly, bait plasmid for PDCD5 (pGBKT7-PDCD5) was transformed in yeast strain Y2H Gold. Transformants containing each bait plasmid were mated with the pre-transformed human Testis cDNA library. From the positive clones showing growth in minimal medium lacking tryptophan, leucine, adenosine, and histidine and with β-galactosidase expression with aureobasidin A selection, plasmids were harvested, prepared, and identified by DNA sequencing.

2.4. RNA isolation and quantitative RT-PCR

Total RNA was extracted using the Trizol reagent following the standard protocol (TAKARA, Shimogyo-ku, Kyoto, Japan). Then, cDNA was prepared using random hexamer primers (Chromogen). PCR was performed using the following forward and reverse primers: 5′-GATGGCAT GGACTGTGGTCA-3′, 5′-GCAATGCCTCCTGCACCACC-3′ (human GAPDH); 5′-GTGGAGAGCATTCCATCCCT-3′, 5′-TGGATGCAGCTTCCTCTCTG-3′ (human CDKN1A); 5′-TCTACTTTGCCAGCAAACTGGTGC-3′, 5′-TGTC CAGCCCATGATGGTTCTGAT-3′ (human BAX); 5′-GTGTTCCTACCCCC AATGTGT-3′, 5′-AGGAGACAACCTGGTCCTCAGT-3′(mouse Gapdh); 5′-GGAGCAGCTTGGGAGCG-3′, 5′-AAAAGGCCCCTGTCTTCATGA-3′ (mouse Bax); and 5′-GCCTTAGCCCTCACTCTGTG-3′, 5′-AGCTGGCC TTAGAGGTGA CA-3′ (mouse Cdkn1a). The concentration of cDNA was normalized using GAPDH. Quantitative-PCR analyses were performed using SYBR Green PCR master mix reagents and an ABI Prism 7700 sequence detection system (Applied Biosystems, Carlsbad, CA, USA). All reactions were performed in triplicate. Relative expression levels and SD values were calculated using the comparative method.

2.5. Adenoviruses and lentiviral shRNAs

For stable knockdown of gene expression, two pairs of oligonucleotides that encode the shRNA against each target MISSION shRNA were purchased (Sigma-Aldrich). To generate lentiviral particles, the pLKO.1-PURO PDCD5 or YAF2 plasmid with three plasmids (pMDLg/pRRE, envelope pRSV-REV and pMD2.G) were co-transfected using lipofectamine 2000 (Invitrogen, Grand Island, NY, USA) into the 293FT cell line. After 48 h incubation, supernatants were collected and filtered using 0.45 μm-pore filters. The HCT116 or A549 cell line was then infected with lentivirus particles. After incubation with virus supernatant for 2 days, cells were selected with 1 μg/ml puromycin (Sigma-Aldrich). Lentivirus PURO shRNA was generated as a control. Recombinant adenoviruses expressing GFP and Cre recombinase were generated as described [31]. These constructs were ligated into an E1 shuttle vector and then linearized with PmeI. The linearized vector was co-transformed into *E. coli* BJ 5183 with the pAdEasy1 vector. All viruses were propagated in 293A cells and purified by CsCl density purification. Viral particles were calculated at 260 nm absorbance. The multiplicity of infection was calculated from viral particle numbers [32].

2.6. Plasmids

Wild-type, full-length PDCD5, YAF2, YAF2-N terminus, and YAF2-C terminus constructs were generated by PCR and cloned into the plasmid vectors pSG5-KF2M1-FLAG, -Myc, or -HA (Sigma-Aldrich), and pGEX4T-1 (GE healthcare, Piscataway, NJ, USA). ATP1B1, ARRDC5,

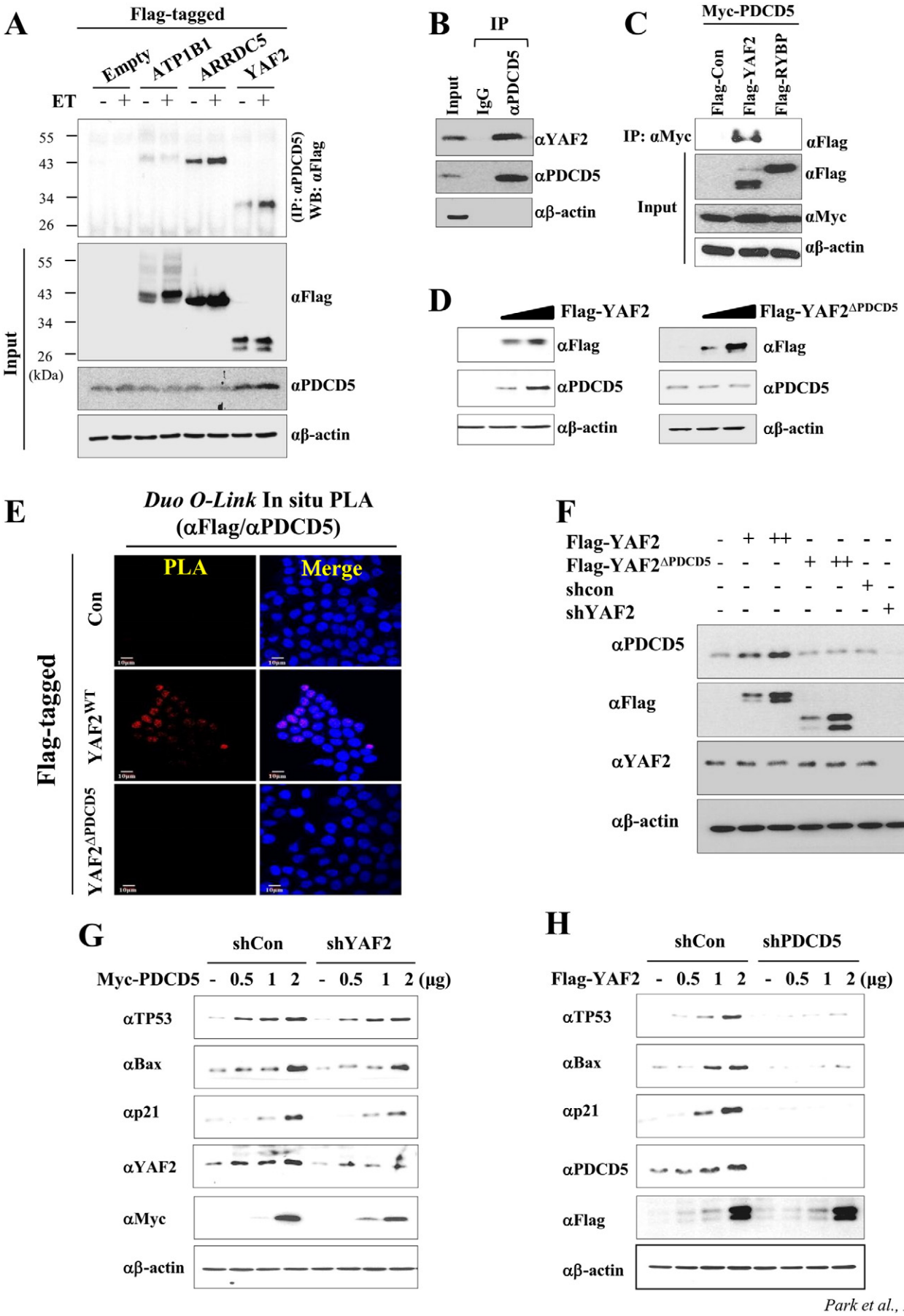

Park et al., Fig. 1

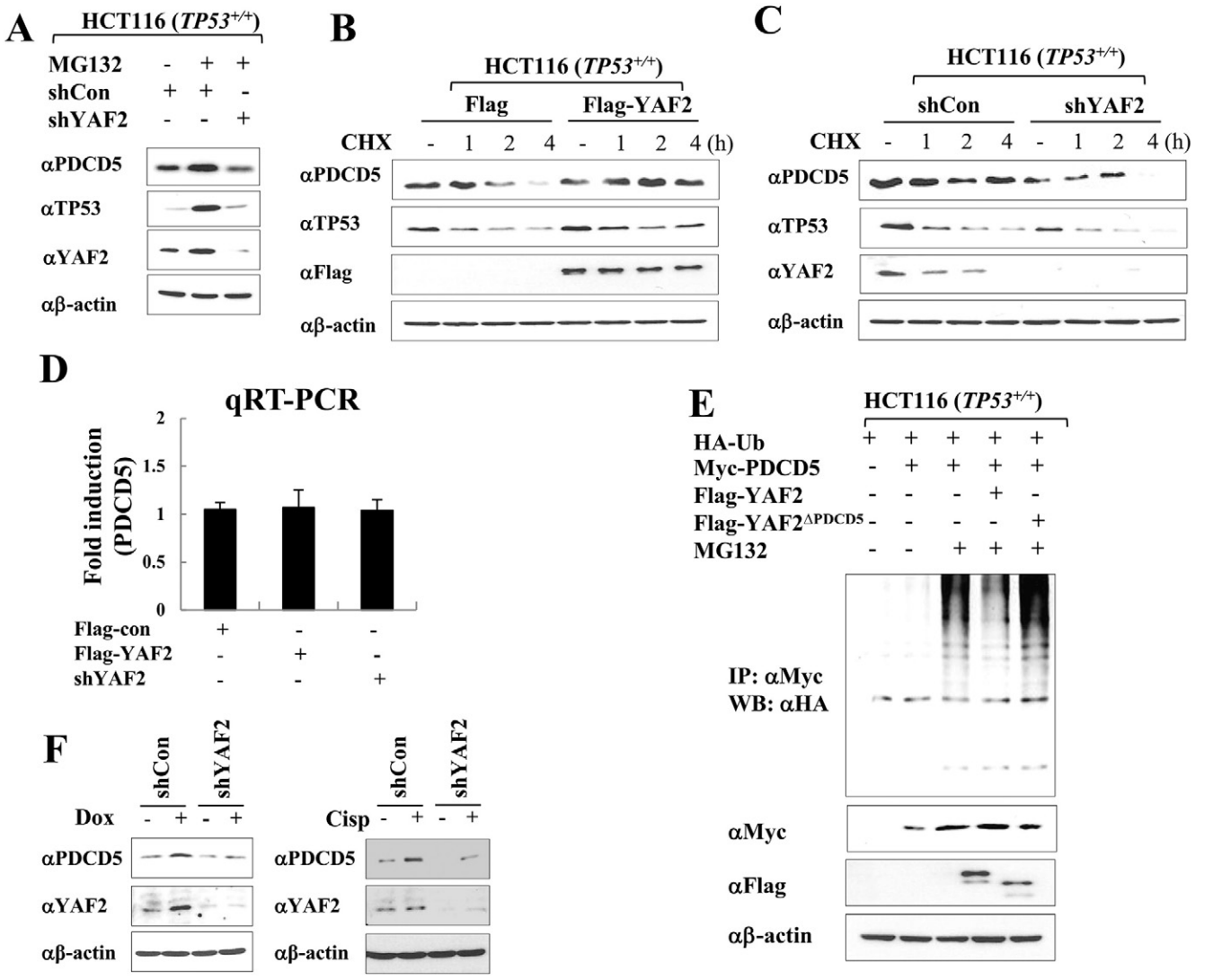

Fig. 2. YAF2 stabilizes PDCD5 in response to genotoxic stress. (A) Knockdown of YAF2 diminishes the effect of MG132 on PDCD5 stability. HCT116 ($TP53^{+/+}$) cells were transfected with MG132 or shYAF2 and immunoblotted with indicated antibodies. Representative blots of three independent experiments are shown. (B) YAF2 increases PDCD5 stability in a TP53-dependent manner. HCT116 ($TP53^{+/+}$) cells were treated with cycloheximide and indicated plasmids for various time periods, and cell lysates were analyzed by Western blotting. Representative blots of three independent experiments are shown. (C) Knockdown of YAF2 reduces PDCD5 stability. HCT116 ($TP53^{+/+}$) cells were treated with cycloheximide and shYAF2 for various time periods, and cell lysates were analyzed by Western blotting. Representative blots of three independent experiments are shown. (D) Overexpression of YAF2 has no effect on mRNA levels of PDCD5. HCT116 cells were transfected with Flag-YAF2 plasmid or shYAF2. The mRNA levels of indicated genes were analyzed by qRT-PCR. The results are shown as means ± SD calculated from three independent experiments. (E) Wild-type YAF2, but not $YAF2^{\Delta PDCD5}$, inhibits the ubiquitination of PDCD5. HCT116 ($TP53^{+/+}$) cells were transfected with the indicated set of plasmids and/or MG132, and cell lysates were analyzed by Western blotting. Representative blots of three independent experiments are shown. (F) Knockdown of YAF2 diminishes PDCD5 and TP53 induction in response to genotoxic stresses. HCT116 cells were transfected with the indicated sets of shRNAs and were stimulated with doxorubicin (50 μM) or cisplatin (50 μM). Dox, doxorubicin; Cisp, cisplatin; ET, etoposide. Representative blots of three independent experiments are shown.

YBX1, STK11IP, NSEP, PDCL3, SYCP1, PCMT1, PLSCR2, UBXN7, WDR74 were obtained from DNASU Plasmid Repository (Arizona University, Tempe, AZ, USA). All plasmid constructs were verified by DNA sequencing.

2.7. Site-direct mutagenesis

Various mutants were created using the QuickChange kit (Agilent Technologies, Santa Clara, CA, USA). PCR cycling conditions used in

Fig. 1. YAF2 binds to and selectively increases PDCD5 protein levels in response to genotoxic stress. (A) YAF2 selectively increases the levels of PDCD5 protein. HCT116 ($TP53^{+/+}$) cells were transfected with the indicated sets of plasmids and were stimulated without or with 50 μM etoposide (ET) for 6 h. The immunoprecipitation assay was carried out with PDCD5 antibody. Representative blots of three independent experiments are shown. (B) Validation of endogenous interactions between PDCD5 and YAF2. Cells were immunoprecipitated with anti-YAF2 or anti-PDCD5 antibody and subsequently immunoblotted with indicated antibodies. Representative blots of three independent experiments are shown. (C) PDCD5 specifically interacts with YAF2, but not its paralog RYBP. Cells were transfected with indicated plasmids. Whole cell lysates were immunoprecipitated with anti-Myc, and subsequently immunoblotted with indicated antibodies. Representative blots of three independent experiments are shown. (D) Wild-type YAF2, but not the PDCD5-interacting defective mutant $YAF2^{\Delta PDCD5}$, increases PDCD5 protein levels. Cells were transfected with the indicated sets of plasmids. Whole cell lysates were immunoblotted with the indicated antibodies. Representative blots of three independent experiments are shown. (E) Validation of interaction between YAF2 and PDCD5. Cells were transfected with the indicated sets of YAF2 plasmids. In situ PLA analysis was performed as described in Materials and methods. Representative images of three independent experiments are shown. Bar scale = 10 μm. (F) Knockdown of YAF2 reduces PDCD5 levels. Cells were transfected with the indicated sets of plasmids or shRNA against YAF2. Representative blots of three independent experiments are shown. (G) PDCD5 overcomes the knockdown effect of YAF2 on TP53 activation. Stable shYAF2-expressing HCT116 cells were transfected with increased amounts of Myc-PDCD5 plasmids and immunoblotted with the indicated set of antibodies. Representative blots of three independent experiments are shown. (H) Knockdown of PDCD5 eliminated the positive effect of YAF2 on TP53 activation. Stable shPDCD5-expressing HCT116 cells were transfected with increased amounts of Flag-YAF2 plasmids and immunoblotted with the indicated set of antibodies. Representative blots of three independent experiments are shown.

site-directed mutagenesis were 18 cycles of amplification with the following reaction: denaturation at 94 °C for 30 s, annealing at 55 °C for 1 min, and extension at 68 °C for 10 min. Amplified mixtures were treated with *Dpn*I (Agilent Technologies) at 37 °C for 1 h and aliquots were used to transform competent *E. coli*. All constructs were confirmed by DNA sequencing.

2.8. In vivo ubiquitination assay

HCT116 cells were co-transfected with HA-Ub plasmid, Myc-PDCD5, and Flag-YAF2. After 48 h, whole cell lysates were treated with MG132 for 6 h and subsequently processed for immunoprecipitation with anti-Myc antibody. Ubiquitination of Myc-PDCD5 was visualized by Western blotting with anti-HA antibody.

2.9. TP53 oligomerization assay

Cells were lysed with lysis buffer and immunoprecipitated with indicated tagged antibody or TP53 antibody with agarose A/G beads (Santa Cruz). Agarose beads were washed with PBS, and glutaraldehyde (Sigma-Aldrich) was added to the immunoprecipitants at indicated concentrations. After incubating for 20 min at 37 °C, the reactions were stopped by adding 2× loading buffer, and the samples were heated at 100 °C for 5 min and resolved by SDS-PAGE. Immunoblot analysis was performed with anti-TP53 or indicated tagged antibody.

2.10. Duo Link in situ proximity ligation assay (PLA)

Duo Link in situ PLA analysis was performed according to the manufacturer's instructions (Sigma-Aldrich). In short, paraformaldehyde-fixed cells were washed with PBS, incubated for 15 min in 1.5% hydrogen peroxide, washed, and blocked with blocking solution. Primary rabbit antibody was applied, and the cells were incubated with PLUS and MINUS secondary PLA probes against rabbit IgG only or against both rabbit and mouse IgG. The incubation was followed by hybridization and ligation, and then amplification was performed. After mounting with Duo Link mounting medium, the samples were examined using a Zeiss LSM700 confocal microscope (Carl Zeiss, Oberkochen, Germany).

2.11. MTT assay

Cell viability was determined with the conventional MTT reduction assay. First, 5×10^3–1×10^4 cells were seeded in a 96-well plate. After overnight incubation, cells were transfected with indicated plasmids for 30 h, and the cells were treated with 50 μM ET for another 48 h. Cells were then treated with 15 μM MTT solution (2 mg/ml) for 90 min at 37 °C, the formation of formazan was resolved with DMSO solution for 30 min with shaking. The absorbance was recorded at 570 nm, and a reference was recorded at 630 nm with a microplate reader (Model 550, BIO-RAD Laboratories, Hercules, CA, USA).

2.12. TUNEL assay

For the detection of apoptosis in cells, DNA fragmentation was evaluated by a TUNEL assay using the HT Titer TACS Assay Kit (Trivigen, Gaithersburg, MD, USA) according to the manufacturer's instructions. Briefly, the cells were fixed with 3.7% buffered formaldehyde solution for 7 min, washed with PBS, permeabilized with 100% methanol for 20 min, washed with PBS twice, digested with proteinase K for 15 min, quenched with 3% hydrogen peroxide, washed with distilled water, labeled with deoxynucleotidyl transferase, incubated at 37 °C for 90 min, and then treated with stop buffer. The cells were incubated with TACS-Sapphire substrate, and the colorimetric reaction was stopped with 0.2 N HCl after 30 min. The colorimetric reaction was measured in a microplate reader at absorbance 450 nm.

2.13. Xenograft experiments

A suspension of 2×10^5 A549 cells in 100 μl PBS was injected subcutaneously into the right flank of 5-week-old athymic BALB/c nu/nu mice (Orient, Seoul, Korea). Each experimental group included eight mice. Tumor size was monitored closely and measured every 7 days using a caliper. Two weeks after injection, mice with comparable-sized tumors (~200 mm^3) were selected for treatment with ET (10 mg/kg) at 2-day intervals for five weeks. After five weeks of ET treatment, mice were sacrificed, and tumors were harvested, photographed, and weighed. The volume of tumors was estimated using the formula: $Volume = ½ \times a \times b2$, where ($a$) and ($b$) represent the largest and smallest diameters, respectively. Animal studies were performed after obtaining approval according to the guidelines of the Institutional Animal Care committee of the Ulsan College of Medicine.

2.14. Statistical analysis

Statistical significance was examined using Student's *t*-tests. The two-sample *t* test was used for two-group comparisons. Values were reported as means ± standard deviations (SD). *P* values < 0.05 were considered significant.

3. Results

3.1. YAF2 selectively binds to and increases PDCD5 protein levels

To explore the regulatory mechanism of PDCD5 function during DNA damage response, we first dissected the PDCD5 interactome using yeast two-hybrid assays. Because an elevated level of PDCD5 mRNA was reported in the mouse testis [15], a human testis cDNA library was used for this analysis (Supplementary Table S1). Among the putative PDCD5-interacting proteins, we found that PDCD5 strongly interacts with four proteins including ATP1B1, ARRDC5, PLSCR2, and YAF2 (Supplementary Fig. S1). Importantly, overexpression of YAF2 selectively increased PDCD5 protein levels in response to etoposide (ET) when compared with other PDCD5-interacting proteins (Fig. 1). We also verified the endogenous interaction between PDCD5 and YAF2 (Fig. 1B).

Fig. 3. YAF2 promotes TP53 activation via PDCD5. (A) Knockdown of YAF2 impairs the induction of PDCD5 and TP53 in response to ET. Cells were transfected with the indicated sets of shRNAs and were stimulated with 50 μM ET. Representative blots of three independent experiments are shown. (B) Co-expression of PDCD5 with YAF2 synergistically enhances the effect of ET on TP53 pathway activation when compared with PDCD5 or YAF2 alone. HCT116 cells were transfected with the indicated set of plasmids and immunoblotted with indicated antibodies. Representative blots of three independent experiments are shown. (C) Association of YAF2 with PDCD5 is required for activation of PDCD5 and TP53 response to ET. HCT116 cells were transfected with the indicated set of plasmids and immunoblotted with indicated antibodies (lower panel). Representative blots of three independent experiments are shown. Levels of indicated genes were analyzed by real-time PCR (upper panel). The results are shown as means ± SD calculated from three independent experiments. (*P < 0.05 vs. −ET; #P < 0.05 vs. with +ET). (D) YAF2 fails to overcome the knockdown effect of PDCD5 on TP53 pathway activation. Stable shPDCD5-expressing HCT116 ($TP53^{+/+}$) cells were transfected with Flag-YAF2 plasmids and immunoblotted with indicated antibodies (lower panel). Representative blots of three independent experiments are shown. Levels of indicated genes were analyzed by real-time PCR (upper panel). The results are shown as means ± SD calculated from three independent experiments. (*P < 0.05 vs. −ET; #P < 0.05, ##P < 0.01 vs. with +ET). (E) PDCD5 overcomes the knockdown effect of YAF2 on TP53 pathway activation. Stable shYAF2-expressing HCT116 ($TP53^{+/+}$) cells were transfected with HA-PDCD5 plasmids and immunoblotted with indicated antibodies (lower panel). Representative blots of three independent experiments are shown. Levels of indicated genes were analyzed by real-time PCR (upper panel). The results are shown as means ± SD calculated from three independent experiments. (*P < 0.05 vs. −ET; #P < 0.05 vs. with +ET; **P < 0.05 vs. +ET + shYAF2).

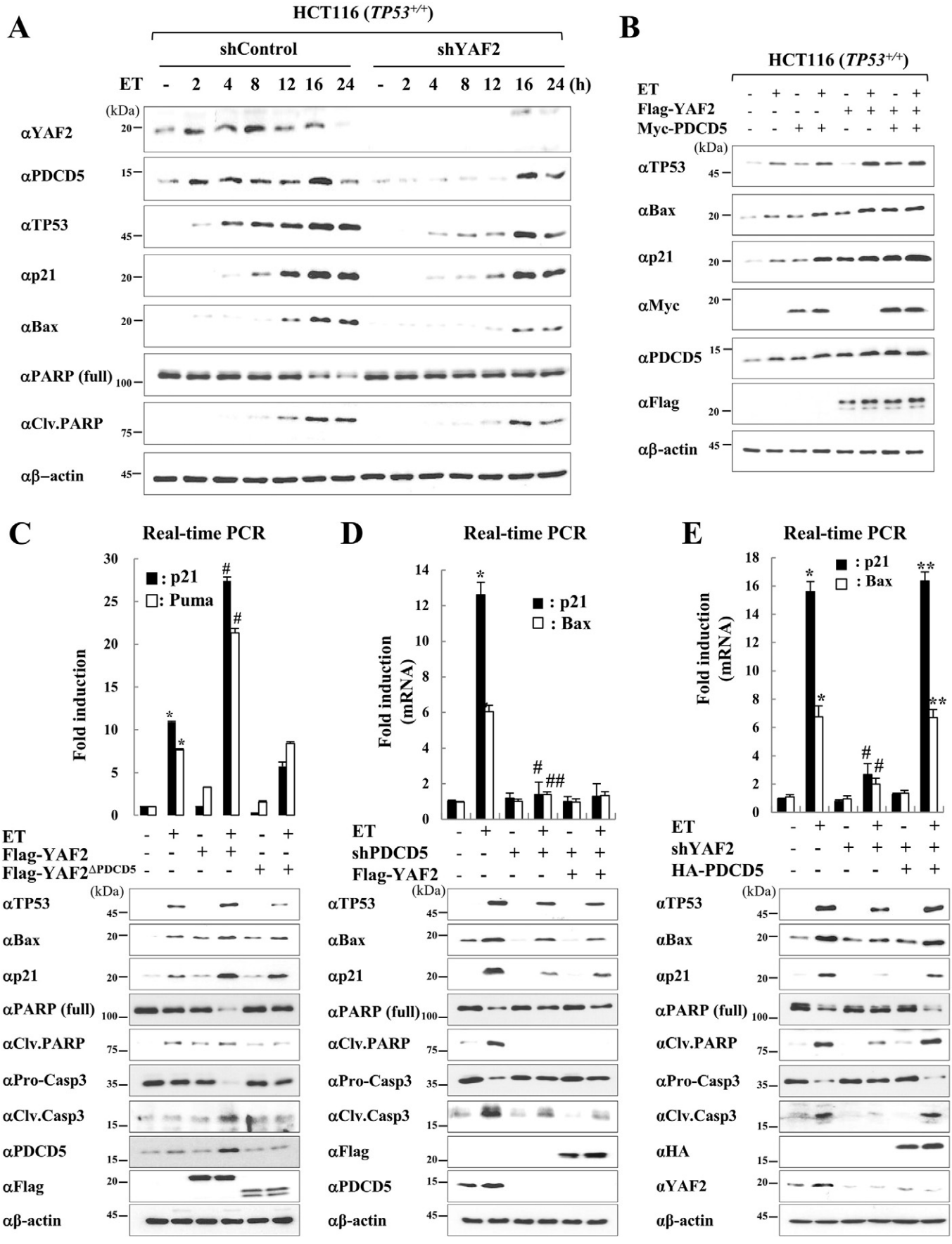
A
HCT116 (TP53+/+)
shControl
shYAF2
ET - 2 4 8 12 16 24 - 2 4 8 12 16 24 (h)
(kDa)
αYAF2
αPDCD5
αTP53
αp21
αBax
αPARP (full)
αClv.PARP
αβ–actin
B
HCT116 (TP53+/+)
ET
Flag-YAF2
Myc-PDCD5
αTP53
αBax
αp21
αMyc
αPDCD5
αFlag
αβ-actin
C
Real-time PCR
Fold induction
■: p21
□: Puma
ET
Flag-YAF2
Flag-YAF2ΔPDCD5
αTP53
αBax
αp21
αPARP (full)
αClv.PARP
αPro-Casp3
αClv.Casp3
αPDCD5
αFlag
αβ-actin
D
Real-time PCR
Fold induction (mRNA)
■: p21
□: Bax
ET
shPDCD5
Flag-YAF2
αTP53
αBax
αp21
αPARP (full)
αClv.PARP
αPro-Casp3
αClv.Casp3
αFlag
αPDCD5
αβ-actin
E
Real-time PCR
Fold induction (mRNA)
■: p21
□: Bax
ET
shYAF2
HA-PDCD5
αTP53
αBax
αp21
αPARP (full)
αClv.PARP
αPro-Casp3
αClv.Casp3
αHA
αYAF2
αβ-actin

PDCD5 specifically interacts with YAF2, but not its paralog RYBP, which was found to participate in apoptosis [33], again verifying a specific interaction between YAF2 and PDCD5 (Fig. 1C). Mapping analysis demonstrated the N-terminal domain (31–60 a.a.) of YAF2 interacted with PDCD5 (Supplementary Fig. S2A). Overexpression of a PDCD5-interaction defective mutant, YAF2$^{\Delta PDCD5}$, had no effect on PDCD5

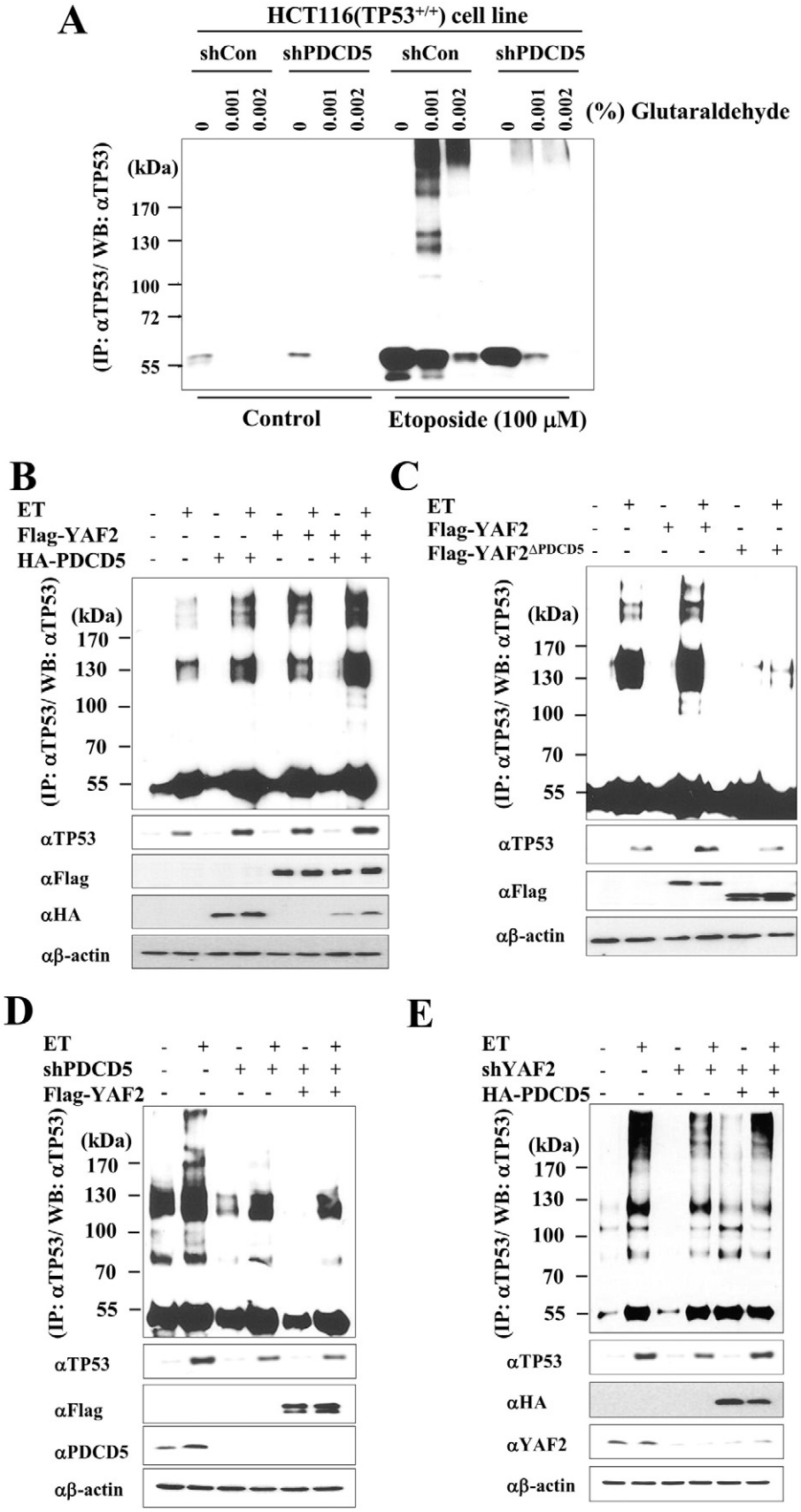

protein levels when compared with wild-type YAF2^{WT}, suggesting the interaction between YAF2 and PDCD5 is required for increased PDCD5 levels (Fig. 1D). Moreover, in situ proximity ligation assay (PLA) analysis again confirmed the interaction between PDCD5 and YAF2 proteins. However, PDCD5 again failed to interact with a PDCD5-interaction defective mutant, YAF2$^{\Delta PDCD5}$ (Fig. 1E). Since overexpression of YAF2 increased PDCD5 protein levels, we next tested the knocking-down effect of YAF2 on PDCD5 protein levels. Knockdown of YAF2 reduced endogenous PDCD5 levels (Fig. 1F). Because PDCD5 levels positively correlated with those of TP53, we next examined the knockdown effect of YAF2 on PDCD5-induced TP53 activation. Interestingly, overexpression of PDCD5 efficiently overcame the knockdown effects of YAF2 on TP53 levels and the expression of TP53 target genes (Fig. 1G). However, knockdown of PDCD5 abrogated the overexpression effect of YAF2 on TP53 activation (Fig. 1H). These data indicate that YAF2 promotes TP53 activation via association with PDCD5.

3.2. YAF2 stabilizes PDCD5 by inhibiting ubiquitination of PDCD5

Because YAF2 enhances PDCD5 expression, we next examined if YAF2 increases the stability of PDCD5 in response to genotoxic stress. Treatment with MG132 efficiently increased PDCD5 levels, whereas the knockdown of YAF2 diminished the effect of MG132 on the stabilization of PDCD5 proteins (Fig. 2A). A time-course experiment with cycloheximide (CHX) treatment showed that YAF2 enhances PDCD5 stability (Fig. 2B). Notably, YAF2 knockdown led to reduced PDCD5 stability, but not reduced PDCD5 mRNA levels, indicating YAF2's critical role in PDCD5 stabilization (Fig. 2C and D). Because overexpression of YAF2 greatly increased PDCD5 protein stability, we next investigated if YAF2 increases PDCD5 stability by inhibiting the ubiquitin-dependent proteosomal degradation pathway. As shown in Fig. 2E, overexpression of wild-type YAF2 substantially reduced the ubiquitination of PDCD5. However, overexpression of mutant YAF2$^{\Delta PDCD5}$ failed to reduce the levels of PDCD5 ubiquitination (Fig. 2E). Furthermore, we also observed that knockdown of YAF2 significantly diminished PDCD5 stabilization by other DNA damage reagents such as doxorubicin and cisplatinin, indicating the common role of YAF2 in genotoxic stress-induced PDCD5 stabilization (Fig. 2F). Collectively, these data suggest that YAF2 stabilizes PDCD5 by inhibiting ubiquitination of PDCD5.

3.3. YAF2 promotes TP53 activation via PDCD5

Because both PDCD5 and TP53 are robustly induced by DNA damage [29], we next investigated if YAF2 expression is also induced by ET treatment. Similar to PDCD5, YAF2 was induced at the early phase of ET treatment when compared with TP53. Interestingly, knockdown of YAF2 greatly delayed the induction of PDCD5 and TP53 response to ET, indicating that YAF2 induction is required for PDCD5 and TP53 activation (Fig. 3A). Importantly, co-expression of PDCD5 with YAF2 synergistically enhanced the effect of ET on TP53 expression when compared with PDCD5 or YAF2 alone (Fig. 3B). However, mutant YAF2$^{\Delta PDCD5}$ failed to enhance the expression and transcriptional activity of TP53 upon ET treatment (Fig. 3C). Since we observed that overexpression of YAF2 failed to overcome the knockdown effect of PDCD5 on TP53 activation, we thus examined if YAF2 promotes TP53-mediated genotoxic stress responses via PDCD5. Overexpression of YAF2 failed to reverse the knockdown effect of PDCD5 on ET-induced TP53 activation (Fig. 3D). However, PDCD5 efficiently overcame the knockdown effect of YAF2 on ET-induced TP53 activation, indicating that YAF2 activates TP53 via PDCD5 (Fig. 3E).

Tetramerization of TP53 is essential for DNA-binding, protein–protein interactions, post-translational modifications, and stabilization of TP53 [34]. We intriguingly found that PDCD5 possesses a putative double-strand DNA-binding domain (8–49 a.a.) by structure analysis of PDCD5 protein using the Conserved Domain Database (NCBI) [35] (Supplementary Fig. S3A). Because YAF2 promotes TP53 stabilization via PDCD5, we tested if YAF2 enhanced ET-induced TP53 tetramerization via PDCD5. Although ET robustly induced TP53 tetramerization, knockdown of PDCD5 fully abrogated ET-induced TP53 tetramerization (Fig. 4A). Co-expression of PDCD5 with YAF2 significantly enhanced ET-induced TP53 tetramerization (Fig. 4B). Importantly, mutant YAF2$^{\Delta PDCD5}$ failed to enhance TP53 tetramerization compared with wild-type YAF2, indicating that YAF2 promotes TP53 tetramerization via association with PDCD5 (Fig. 4C). Furthermore, knockdown of PDCD5 abolished the overexpression effect of YAF2 on ET-induced TP53 tetramerization (Fig. 4D). Conversely, overexpression of PDCD5 efficiently reversed the knockdown effect of YAF2 on ET-induced TP53 tetramerization (Fig. 4E). Collectively, these data indicate that YAF2 promotes TP53-mediated genotoxic stress responses via PDCD5.

3.4. Depletion of PDCD5 abrogates YAF2-mediated TP53 activation

We further validated our findings using *Pdcd5-depleted* mouse embryonic fibroblast (MEF) cells by generating Pdcd5$^{flox/flox}$ mice (Supplementary Fig. S3). Fibroblasts generated from these mice were subjected to adenovirus-expressing Cre recombinase (Ad-Cre) infection to delete PDCD5 and to generate Pdcd5$^{-/-}$ MEFs. As expected, ET treatment failed to induce TP53 stabilization and activation in Pdcd5$^{-/-}$ MEF cells compared with Pdcd5$^{+/+}$ MEF cells (Fig. 5A). Although YAF2 enhanced ET-induced PDCD5 stabilization and TP53 activation, genetic depletion of PDCD5 reversed the positive action of YAF2 on PDCD5 stabilization (Fig. 5A). Conversely, reintroduction of PDCD5 in Pdcd5$^{-/-}$ MEF cells dramatically restored YAF2 function in promoting TP53 activation (Fig. 5B). To further validate the functional importance of PDCD5 in TP53 activation, we assessed the activity of well-known TP53 activators in the presence or absence of PDCD5. ET failed to increase TP53 activation in the absence of PDCD5. Importantly, the dissociation of MDM2 from TP53 by nutlin-3a had a negligible effect on TP53 activation in the absence of PDCD5, indicating that PDCD5 is required for TP53 activation. Moreover, treatment with another TP53 activator, tenovin-6, displayed the same result as nutlin-3a and ET treatment (Fig. 5C). As we mentioned above, PDCD5 possesses a putative DNA binding domain and its knocking-down impaired TP53 tetramerization in response to ET, we next explored the possibility that PDCD5 mediates TP53 recruitment to the promoter region of target genes. We performed chromatin immunoprecipitation (ChIP) analyses of the TP53-binding site (TP53-RE) on *Bax*, which showed that the restoration of PDCD5 in Pdcd5$^{-/-}$ MEF cells rescued the ET-induced recruitment of the TP53-p300 complex to the TP53-binding site of its target genes. However,

Fig. 4. YAF2 enhances the TP53 oligomerization via PDCD5. (A) Knocking-down of PDCD5 diminishes TP53 oligomerization in response to ET treatment. Stable shPDCD5-expressing HCT116 (TP53$^{+/+}$) cells were transfected with indicated plasmids and immunoblotted with the respective antibodies. For TP53 oligomerization assays, the same amounts of proteins were immunoprecipitated with anti-TP53 antibody. Immunoprecipitants were washed with PBS and cross-linked using 0.001% glutaraldehyde. Oligomerization of TP53 was analyzed by immunoblotting with anti-TP53 antibody. Representative blots of three independent experiments are shown. (B) Synergistic effect of PDCD5 and YAF2 on the etoposide (ET)-induced oligomerization of TP53. HCT116 cells were transfected with indicated plasmids and treated with ET for 6 h. Whole cell lysates were immunoprecipitated with anti-TP53 antibody and cross-linked using 0.01% glutaraldehyde. The oligomerization of TP53 was analyzed by immunoblotting with anti-TP53 antibody. Representative blots of three independent experiments are shown. (C) Overexpression of wild-type YAF2, but not of mutant YAF2$^{\Delta PDCD5}$, enhances ET-induced oligomerization of TP53. The oligomerization of TP53 was analyzed as described above. Representative blots of three independent experiments are shown. (D) Knockdown of PDCD5 abrogates the enhancing action of YAF2 on ET-induced TP53 oligomerization. Stable shPDCD5-expressing HCT116 cells were transfected with the Flag-YAF2 plasmid. The oligomerization of TP53 was analyzed as described above. Representative blots of three independent experiments are shown. (E) PDCD5 overcomes the knockdown effect of YAF2 on TP53 oligomerization. The oligomerization of TP53 was analyzed by immunoblotting with anti-TP53 antibody. Representative blots of three independent experiments are shown.

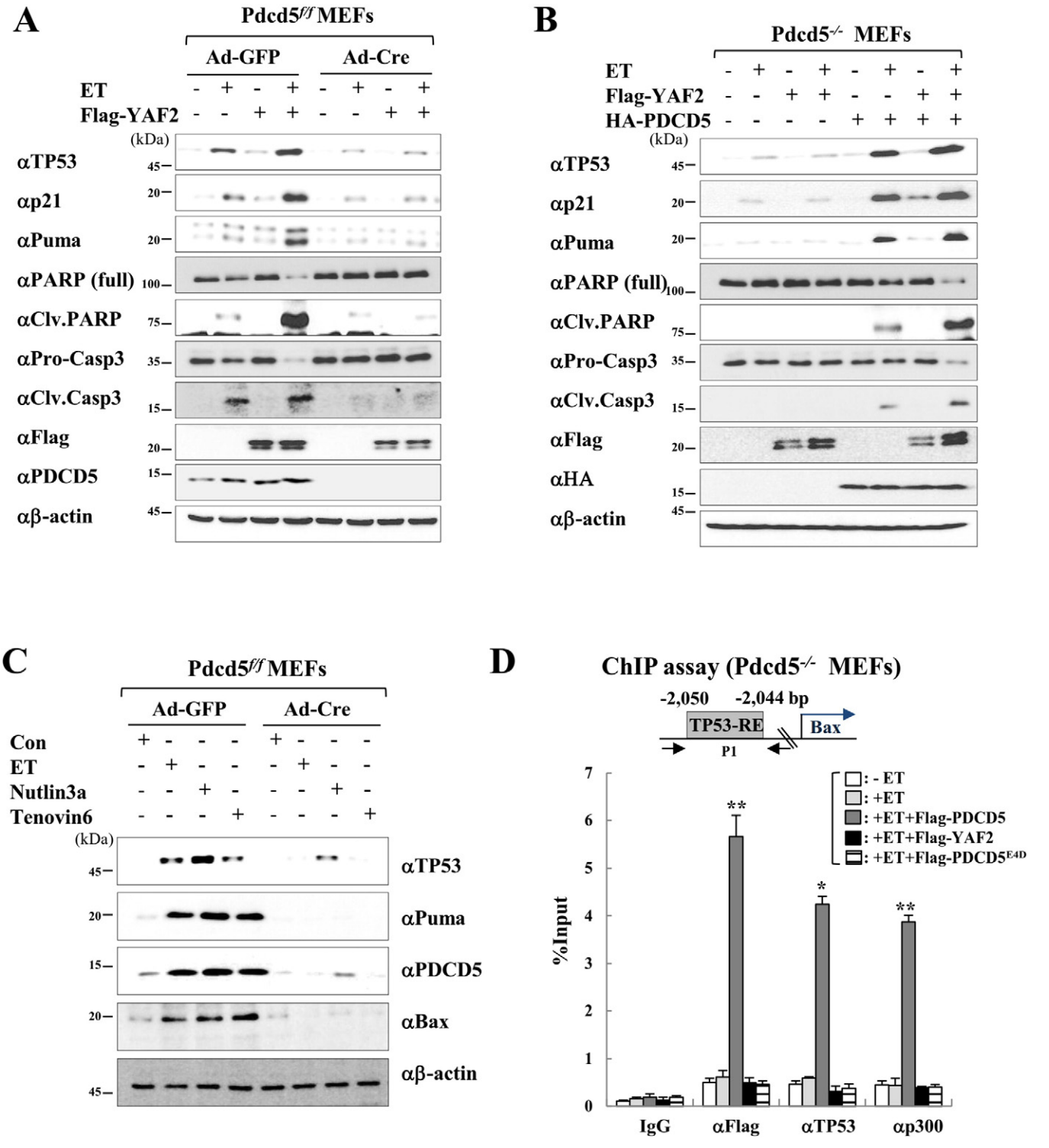

Fig. 5. Depletion of PDCD5 eliminates YAF2-mediated TP53 activation. (A) Depletion of PDCD5 abrogates the effect of YAF2 on etoposide (ET)-induced TP53 activation. Pdcd5$^{f/f}$ MEF cells following infection with either Ad-Cre or Ad-GFP were established and electroporated with the Flag-YAF2 plasmid. After 24 h, MEF cells were treated with 50 μM ET and subjected to immunoblotting with indicated antibodies. Control undeleted cells are denoted Pdcd5$^{f/f}$, and Pdcd5-deleted cells are denoted Pdcd5$^{-/-}$. Representative blots of three independent experiments are shown. (B) Restoration of PDCD5 returns the function of YAF2 in promoting TP53 activation. Pdcd5$^{-/-}$ MEF cells were electroporated with indicated plasmids and treated with ET. Whole cell lysates were immunoprecipitated with indicated antibodies. Representative blots of three independent experiments are shown. (C) PDCD5 is required for TP53 activation in response to multiple TP53 activators. Pdcd5$^{f/f}$ MEF cells following infection with either Ad-Cre or Ad-GFP were established and treated with indicated TP53 activators (ET: 50 μM; Nutlin-3a: 10 μM; Teonovin-6: 10 μM). Representative blots of three independent experiments are shown. (D) Restoration of PDCD5 induces recruitment of the TP53-p300 complex to the promoter region of Bax in response to ET. Pdcd5$^{-/-}$ MEF cells were electroporated with indicated plasmids and then treated with ET. ChIP assays were performed with the indicated antibodies. Precipitated samples were analyzed by real-time PCR, and results are presented as the percentage of input. The results are shown as means ± SD calculated from three independent experiments. (*$P < 0.05$, **$P < 0.01$ vs. + ET).

restoration of YAF2 or YAF2-interaction defective point mutant, PDCD5$^{\Delta YAF2}$ had no effect on TP53 recruitment to target genes in the absence of PDCD5, suggesting that PDCD5 mediates TP53 tetramer recruitment to pro-apoptotic genes upon genotoxic stress (Fig. 5D and Supplementary Fig. S2B). Interestingly, Flag-tagged PDCD5, but not YAF2, was recruited to the TP53-binding site of target genes with TP53 and p300. Taken together, these results indicate PDCD5 is required for TP53-mediated transcriptional activation of pro-apoptotic genes.

3.5. YAF2 facilitates in vivo genotoxic stress responses in a PDCD5-dependent way

To corroborate the crucial role of PDCD5 in genotoxic stress-induced apoptosis, we performed a TUNEL assay in the knockdown of PDCD5 and found ET treatment dramatically increased DNA damage, although knockdown of PDCD5 diminished the effect of ET on apoptosis of A549 cells. YAF2 failed to restore the inhibitory effect of ET on the growth of A549 cells in the PDCD5 knockdown (Fig. 6A), but PDCD5 efficiently overcame the knockdown effect of YAF2 on ET-induced apoptosis of A549 cells (Fig. 6B). We next examined the functional consequences of the YAF2-PDCD5 network regarding tumorigenic growth of cancer cells. In response to ET treatment, the growth of A549 lung cancer cells was greatly suppressed; however, knockdown of PDCD5 diminished the effect of ET on the suppression of A549 cancer cell growth. YAF2 failed to restore the inhibitory effect of ET on the growth of A549 cells in the PDCD5 knockdown (Fig. 6C). Conversely, PDCD5 efficiently overcame the knockdown effect of YAF2 on ET-induced suppression of A549 cell growth (Fig. 6D).

Finally, to solidify our finding, we performed reconstitution experiments after generating the TP53-interacting, PDCD5-defective mutant and the YAF2-interacting, PDCD5-defective mutant. Based on the mapping analysis among PDCD5, YAF2, and TP53, we next generated various PDCD5 point mutants by site-directed mutagenesis (Supplementary Fig. S3A). Each myc-tagged PDCD5 point mutant was co-transfected with Flag-YAF2 or Flag-TP53, and then each PDCD5-defective mutant was screened by immunoprecipitation analysis. Notably, each PDCD5-defective mutant selectively failed to interact with the respective proteins (Supplementary Fig. S3B). ET had no effect on cell viability and DNA damage in Pdcd5-depleted MEFs; however, restoration of PDCD5^{WT} in Pdcd5$^{-/-}$ MEF cells led to substantial genotoxic stress-induced DNA damage. Importantly, restoration of PDCD5$^{E16D(TP53)}$ and PDCD5$^{E16D(YAF2)}$ did not induce the DNA damage and cell death, verifying the apoptotic signaling cascade consists of YAF2, PDCD5, and TP53 (Fig. 6E). Furthermore, in vivo tumorigenicity assays using subcutaneous injection of A549 cells into nude mice demonstrated that reduction of PDCD5 significantly enhanced the chemoresistance of A549 cells. However, restoration of wild-type PDCD5, but not of PDCD5-^{E16D} or PDCD5^{E16D}, markedly reversed the chemoresistance of PDCD5-depleted A549 cells (Fig. 6F). These data collectively demonstrate that the YAF2 facilitates genotoxic stress response via PDCD5.

4. Discussion

Imbalanced levels of intracellular apoptotic proteins are common in cancer cells. Therefore, understanding apoptosis signaling proteins in cancer cells may lead to the development of potential anticancer strategies. In our present study, we identified YAF2 as PDCD5-interacting partner. The YAF2 protein was originally identified as the binding partner of Yin-Yang-1 (YY-1) transcriptional factor with YY-1 and E4TF1/hGABP-associated factor-1 [36]. According to a yeast three-hybrid assay, YAF2 positively regulates the transcriptional activity of E4TF1, a sequence-specific transcription factor, that regulates cytochrome c oxidative subunits IV and Vb, the ATP synthase β-subunit, ribosomal proteins L30 and L32, and the retinoblastoma tumor suppressor proteins [37]. In addition, YAF2 is a proto-oncogene Myc- and MycN-associated protein and inhibits Myc-mediated transactivation and transformation [38]. These results collectively demonstrate the crucial roles of YAF2 as a cofactor during transcriptional regulation. Conversely, limited information exists related to the role of YAF2 during apoptosis. During zebrafish embryogenesis, YAF2 inhibited caspase-8-mediated apoptosis and induced cell survival [39], but we here found much evidence that YAF2 acts as a pro-apoptotic regulator in cancer cells. First, YAF2 was robustly induced and interacts with PDCD5 in response to ET. Second, knockdown of YAF2 greatly diminished genotoxic stress-induced PDCD5 stabilization and TP53 activation. Third, YAF2 enhanced the activation of TP53 and cellular apoptosis via PDCD5. The RYBP (RING1 and YY-1 binding protein) is a human paralog of YAF2 and has a functional form distinct from YAF2 during its transcriptional regulation of Polycomb target genes [40]. In addition to a transcription factor, RYBP inhibits ubiquitination and degradation of TP53 via interaction with MDM2 [33]. In our study, we observed a similar action of YAF2 by its mediation of PDCD5 and TP53 interaction during apoptosis. Considering the functional differences of the two homologs, both YAF2 and RYBP may form different protein complexes during apoptosis. With regard to this possibility, we verified that PDCD5 selectively interacts with YAF2 but not with RYBP. Based on these findings, we suggest that YAF2 acts as an apoptosis-facilitating molecule by mediating protein–protein interaction upon genotoxic stress.

TP53 is known to mediate cell fate decision depending on the intensity of stress between survival and death. Upon DNA damage, TP53 arrests the cell cycle and facilitates DNA repair. If the damage is beyond repair, TP53 promotes the expression of pro-apoptotic genes such as Bax and Puma to trigger apoptosis. For TP53-mediated cell fate decision, diverse TP53 cofactors such as HIPK2, DYRK2, PCAF, and E4F1 are involved in the decision-making process [41]. Thus, TP53 make cell fate decision upon cellular stresses, at least in part, through interaction with specific cofactors. It has been shown that PDCD5 is rapidly upregulated and translocated into nucleus to promote DNA damage response [28]. Based on our time-course experiments, both YAF2 and PDCD5 are induced at the early phase of ET treatment (2 h) when compared to TP53. Knocking-down of either YAF2 or PDCD5 greatly reduced the TP53 activation in a response to genotoxic stress. Moreover, ChIP assays displayed that PDCD5 is recruited to the promoter region of BAX with TP53. Thus, it is likely that the stabilization of PDCD5 by YAF2 may occur before TP53 stabilization, and then nuclear localized PDCD5 interacts with TP53 to facilitate apoptosis upon prolonged genotoxic stress. Further work would be necessary to determine the specific molecular dynamics among YAF2, PDCD5, and TP53 during genotoxic stress responses.

In summary, we have described the molecular mechanism by which the YAF2 positively regulates PDCD5 function upon genotoxic stress responses. In this pathway, YAF2 stabilizes PDCD5 by inhibiting the ubiquitin-dependent proteosomal degradation pathway, which subsequently leads to TP53 activation. Importantly, we found that YAF2 promotes the TP53 pathway in a PDCD5-dependent manner, highlighting the critical role of PDCD5 in TP53-mediated genotoxic stress responses (Fig. 6G). Our findings reveal a previously undiscovered PDCD5 network that acts as a central hub in the regulation of genotoxic stress responses. Thus, alteration of this PDCD5 network in cancer cells might contribute to tumorigenesis. Further understanding of the clinical relevance of this YAF2-PDCD5 cascade to human tumorigenesis may provide a potential promising target for cancer therapy.

Transparency Document

Transparency Document associated with this article can be found, in the online version.

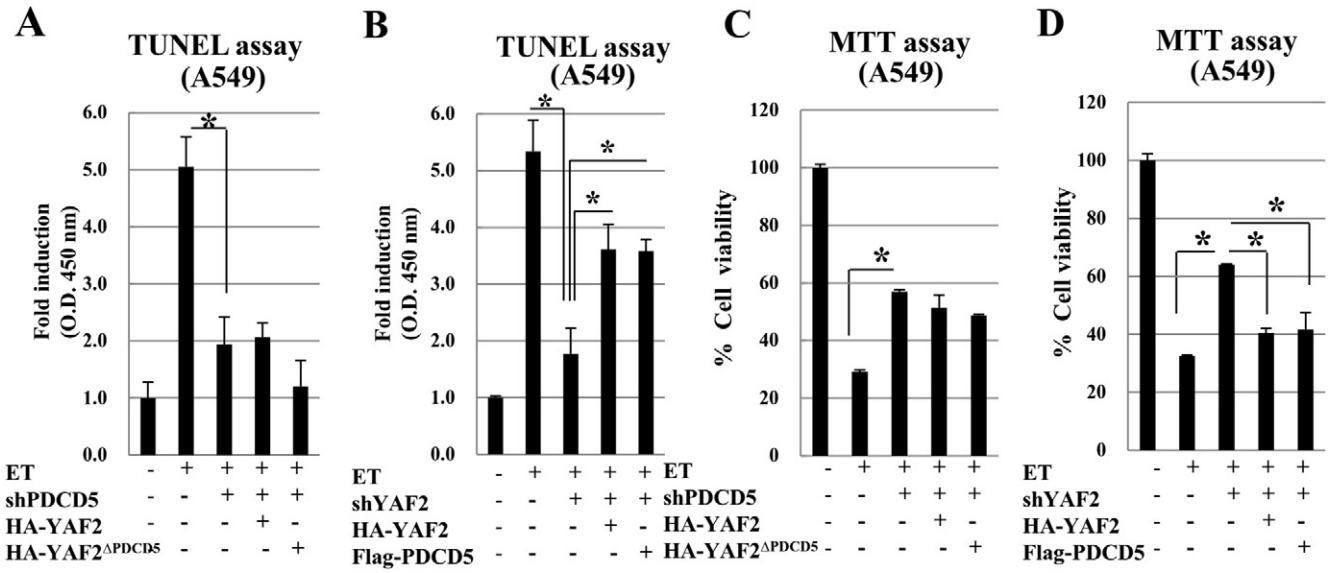
A
TUNEL assay (A549)
Fold induction (O.D. 450 nm)
ET
shPDCD5
HA-YAF2
HA-YAF2ΔPDCD5
B
TUNEL assay (A549)
Fold induction (O.D. 450 nm)
ET
shYAF2
HA-YAF2
Flag-PDCD5
C
MTT assay (A549)
% Cell viability
ET
shPDCD5
HA-YAF2
HA-YAF2ΔPDCD5
D
MTT assay (A549)
% Cell viability
ET
shYAF2
HA-YAF2
Flag-PDCD5

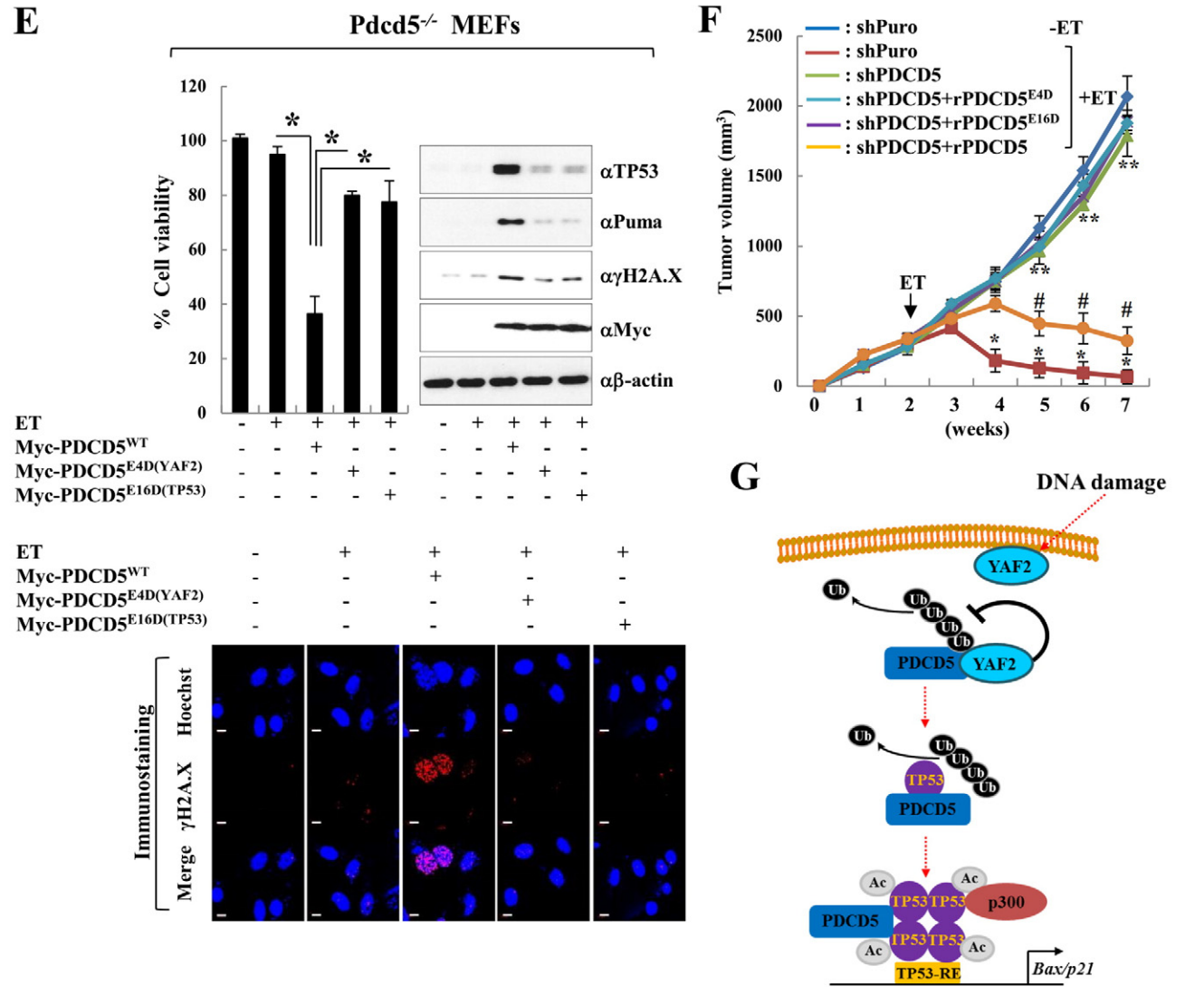
E
Pdcd5-/- MEFs
% Cell viability
αTP53
αPuma
αγH2A.X
αMyc
αβ-actin
ET
Myc-PDCD5WT
Myc-PDCD5E4D(YAF2)
Myc-PDCD5E16D(TP53)
Immunostaining
Hoechst
γH2A.X
Merge
F
: shPuro
: shPuro
: shPDCD5
: shPDCD5+rPDCD5E4D
: shPDCD5+rPDCD5E16D
: shPDCD5+rPDCD5
-ET
+ET
Tumor volume (mm3)
ET
(weeks)
G
DNA damage
YAF2
Ub
PDCD5
YAF2
TP53
PDCD5
Ac
TP53
p300
PDCD5
TP53-RE
Bax/p21

Acknowledgements

This research was supported by Basic Science Research Program through the National Research Foundation of Korea (NRF) funded by the Ministry of Education (NRF-2012R1A6A3A04041010) (H.K. Choi) and by the National Research Foundation of Korea (NRF) grant funded by the Korean Government (MSIP) (No. NRF-2012R1A2A1A01001862 & NRF-2011-0030086) (H.G. Yoon). The authors thank D. S. Jang for his excellent support with medical illustrations.

Appendix A. Supplementary data

Supplementary data to this article can be found online at http://dx.doi.org/10.1016/j.bbamcr.2015.01.006.

References

[1] B. Vogelstein, D. Lane, A.J. Levine, Surfing the p53 network, Nature 408 (2000) 307–310.
[2] C. Dai, W. Gu, p53 post-translational modification: deregulated in tumorigenesis, Trends Mol. Med. 16 (2010) 528–536.
[3] A.M. Bode, Z. Dong, Post-translational modification of p53 in tumorigenesis, Nat. Rev. Cancer 4 (2004) 793–805.
[4] M.H. Kubbutat, S.N. Jones, K.H. Vousden, Regulation of p53 stability by Mdm2, Nature 387 (1997) 299–303.
[5] R.P. Leng, Y. Lin, W. Ma, H. Wu, B. Lemmers, S. Chung, J.M. Parant, G. Lozano, R. Hakem, S. Benchimol, Pirh2, a p53-induced ubiquitin-protein ligase, promotes p53 degradation, Cell 112 (2003) 779–791.
[6] D. Dornan, I. Wertz, H. Shimizu, D. Arnott, G.D. Frantz, P. Dowd, K. O'Rourke, H. Koeppen, V.M. Dixit, The ubiquitin ligase COP1 is a critical negative regulator of p53, Nature 429 (2004) 86–92.
[7] X. Zhang, F.G. Berger, J. Yang, X. Lu, USP4 inhibits p53 through deubiquitinating and stabilizing ARF-BP1, EMBO J. 30 (2011) 2177–2189.
[8] M.L. Avantaggiati, V. Ogryzko, K. Gardner, A. Giordano, A.S. Levine, K. Kelly, Recruitment of p300/CBP in p53-dependent signal pathways, Cell 89 (1997) 1175–1184.
[9] Y. Nakamura, ATM: the p53 booster, Nat. Med. 4 (1998) 1231–1232.
[10] V. Di Stefano, G. Blandino, A. Sacchi, S. Soddu, G. D'Orazi, HIPK2 neutralizes MDM2 inhibition rescuing p53 transcriptional activity and apoptotic function, Oncogene 23 (2004) 5185–5192.
[11] A. Shvarts, W.T. Steegenga, N. Riteco, T. van Laar, P. Dekker, M. Bazuine, R.C. van Ham, W. van der Houven van Oordt, G. Hateboer, A.J. van der Eb, A.G. Jochemsen, MDMX: a novel p53-binding protein with some functional properties of MDM2, EMBO J. 15 (1996) 5349–5357.
[12] Y.S. Chang, B. Graves, V. Guerlavais, C. Tovar, K. Packman, K.H. To, K.A. Olson, K. Kesavan, P. Gangurde, A. Mukherjee, T. Baker, K. Darlak, C. Elkin, Z. Filipovic, F.Z. Qureshi, H. Cai, P. Berry, E. Feyfant, X.E. Shi, J. Horstick, D.A. Annis, A.M. Manning, N. Fotouhi, H. Nash, L.T. Vassilev, T.K. Sawyer, Stapled alpha-helical peptide drug development: a potent dual inhibitor of MDM2 and MDMX for p53-dependent cancer therapy, Proc. Natl. Acad. Sci. U. S. A. 110 (2013) E3445–E3454.
[13] L.T. Vassilev, B.T. Vu, B. Graves, D. Carvajal, F. Podlaski, Z. Filipovic, N. Kong, U. Kammlott, C. Lukacs, C. Klein, N. Fotouhi, E.A. Liu, In vivo activation of the p53 pathway by small-molecule antagonists of MDM2, Science 303 (2004) 844–848.
[14] K. Ding, Y. Lu, Z. Nikolovska-Coleska, S. Qiu, Y. Ding, W. Gao, J. Stuckey, K. Krajewski, P.P. Roller, Y. Tomita, D.A. Parrish, J.R. Deschamps, S. Wang, Structure-based design of potent non-peptide MDM2 inhibitors, J. Am. Chem. Soc. 127 (2005) 10130–10131.
[15] H. Liu, Y. Wang, Y. Zhang, Q. Song, C. Di, G. Chen, J. Tang, D. Ma, TFAR19, a novel apoptosis-related gene cloned from human leukemia cell line TF-1, could enhance apoptosis of some tumor cells induced by growth factor withdrawal, Biochem. Biophys. Res. Commun. 254 (1999) 203–210.
[16] J. Xiao, C. Liu, G. Li, S. Peng, J. Hu, L. Qu, P. Lv, Y. Zhang, D. Ma, Y. Chen, PDCD5 negatively regulates autoimmunity by upregulating FOXP3(+) regulatory T cells and suppressing Th17 and Th1 responses, J. Autoimmun. 47 (2013) 34–44.
[17] P. Zhang, M. Zhao, G. Liang, G. Yin, D. Huang, F. Su, H. Zhai, L. Wang, Y. Su, Q. Lu, Whole-genome DNA methylation in skin lesions from patients with psoriasis vulgaris, J. Autoimmun. 41 (2013) 17–24.
[18] Y. Chen, R. Sun, W. Han, Y. Zhang, Q. Song, C. Di, D. Ma, Nuclear translocation of PDCD5 (TFAR19): an early signal for apoptosis? FEBS Lett. 509 (2001) 191–196.
[19] G.R. Ruan, H.S. Zhao, Y. Chang, J.L. Li, Y.Z. Qin, Y.R. Liu, S.S. Chen, X.J. Huang, Adenovirus-mediated PDCD5 gene transfer sensitizes K562 cells to apoptosis induced by idarubicin in vitro and in vivo, Apoptosis 13 (2008) 641–648.
[20] C. Chen, H. Zhou, L. Xu, D. Xu, Y. Wang, Y. Zhang, X. Liu, Z. Liu, D. Ma, Q. Ma, Y. Chen, Recombinant human PDCD5 sensitizes chondrosarcomas to cisplatin chemotherapy in vitro and in vivo, Apoptosis 15 (2010) 805–813.
[21] X. Ma, G. Ruan, Y. Wang, Q. Li, P. Zhu, Y.Z. Qin, J.L. Li, Y.R. Liu, D. Ma, H. Zhao, Two single-nucleotide polymorphisms with linkage disequilibrium in the human programmed cell death 5 gene 5′ regulatory region affect promoter activity and the susceptibility of chronic myelogenous leukemia in Chinese population, Clin. Cancer Res. 11 (2005) 8592–8599.
[22] M. Spinola, P. Meyer, S. Kammerer, F.S. Falvella, M.B. Boettger, C.R. Hoyal, C. Pignatiello, R. Fischer, R.B. Roth, U. Pastorino, K. Haeussinger, M.R. Nelson, R. Dierkesmann, T.A. Dragani, A. Braun, Association of the PDCD5 locus with lung cancer risk and prognosis in smokers, J. Clin. Oncol. 24 (2006) 1672–1678.
[23] J. Sudbo, A. Reith, O.C. Lingjaerde, Gene-expression profiles in hereditary breast cancer, N. Engl. J. Med. 344 (2001) 2029.
[24] D.Z. Fu, Y. Cheng, H. He, H.Y. Liu, Y.F. Liu, PDCD5 expression predicts a favorable outcome in patients with hepatocellular carcinoma, Int. J. Oncol. 43 (2013) 821–830.
[25] Y.H. Yang, M. Zhao, W.M. Li, Y.Y. Lu, Y.Y. Chen, B. Kang, Y.Y. Lu, Expression of programmed cell death 5 gene involves in regulation of apoptosis in gastric tumor cells, Apoptosis 11 (2006) 993–1001.
[26] H. Li, Q. Wang, F. Gao, F. Zhu, X. Wang, C. Zhou, C. Liu, Y. Chen, C. Ma, W. Sun, L. Zhang, Reduced expression of PDCD5 is associated with high-grade astrocytic gliomas, Oncol. Rep. 20 (2008) 573–579.
[27] X. Zhang, X. Wang, X. Song, Z. Wei, C. Zhou, F. Zhu, Q. Wang, C. Ma, L. Zhang, Clinical and prognostic significance of lost or decreased PDCD5 expression in human epithelial ovarian carcinomas, Oncol. Rep. 25 (2011) 353–358.
[28] L. Xu, Y. Chen, Q. Song, D. Xu, Y. Wang, D. Ma, PDCD5 interacts with Tip60 and functions as a cooperator in acetyltransferase activity and DNA damage-induced apoptosis, Neoplasia 11 (2009) 345–354.
[29] L. Xu, J. Hu, Y. Zhao, J. Hu, J. Xiao, Y. Wang, D. Ma, Y. Chen, PDCD5 interacts with p53 and functions as a positive regulator in the p53 pathway, Apoptosis 17 (2012) 1235–1245.
[30] X. Cui, H.K. Choi, Y.S. Choi, S.Y. Park, G.J. Sung, Y.H. Lee, J. Lee, W.J. Jun, K. Kim, K.C. Choi, H.G. Yoon, DNAJB1 destabilizes PDCD5 to suppress p53-mediated apoptosis, Cancer Lett. 357 (2015) 307–315.
[31] Y.J. Lee, E.H. Ko, J.E. Kim, E. Kim, H. Lee, H. Choi, J.H. Yu, H.J. Kim, J.K. Seong, K.S. Kim, J.W. Kim, Nuclear receptor PPARgamma-regulated monoacylglycerol O-acyltransferase 1 (MGAT1) expression is responsible for the lipid accumulation in diet-induced hepatic steatosis, Proc. Natl. Acad. Sci. U. S. A. 109 (2012) 13656–13661.
[32] J. Luo, Z.L. Deng, X. Luo, N. Tang, W.X. Song, J. Chen, K.A. Sharff, H.H. Luu, R.C. Haydon, K.W. Kinzler, B. Vogelstein, T.C. He, A protocol for rapid generation of recombinant adenoviruses using the AdEasy system, Nat. Protoc. 2 (2007) 1236–1247.
[33] D. Chen, J. Zhang, M. Li, E.R. Rayburn, H. Wang, R. Zhang, RYBP stabilizes p53 by modulating MDM2, EMBO Rep. 10 (2009) 166–172.
[34] T.D. Halazonetis, A.N. Kandil, Conformational shifts propagate from the oligomerization domain of p53 to its tetrameric DNA binding domain and restore DNA binding to select p53 mutants, EMBO J. 12 (1993) 5057–5064.
[35] D. Christendat, A. Yee, A. Dharamsi, Y. Kluger, A. Savchenko, J.R. Cort, V. Booth, C.D. Mackereth, V. Saridakis, I. Ekiel, G. Kozlov, K.L. Maxwell, N. Wu, L.P. McIntosh, K. Gehring, M.A. Kennedy, A.R. Davidson, E.F. Pai, M. Gerstein, A.M. Edwards, C.H. Arrowsmith, Structural proteomics of an archaeon, Nat. Struct. Biol. 7 (2000) 903–909.
[36] C. Sawa, T. Yoshikawa, F. Matsuda-Suzuki, S. Delehouzee, M. Goto, H. Watanabe, J. Sawada, K. Kataoka, H. Handa, YEAF1/RYBP and YAF-2 are functionally distinct members of a cofactor family for the YY1 and E4TF1/hGABP transcription factors, J. Biol. Chem. 277 (2002) 22484–22490.

Fig. 6. YAF2 promotes in vivo genotoxic stress response via PDCD5. (A&C) YAF2 fails to enhance apoptosis in the absence of PDCD5. Stable shPDCD5-expressing A549 cells were transfected with the indicated set of plasmids and treated with 50 μM etoposide (ET). Apoptotic cells were measured by the TUNEL assay. (A). Cell viability was assessed by the MTT assay (C). The results are shown as means ± SD calculated from four independent experiments. *, $P < 0.05$. (B&D) PDCD5 overcome the knockdown effect of YAF2 on ET-induced apoptosis. Stable shYAF2-expressing A549 cells were transfected with the indicated set of plasmids. Apoptotic cells were measured by the TUNEL assay (B). Cell viability was assessed by the MTT assay (D). The results are shown as means ± SD calculated from four independent experiments. *, $P < 0.05$. (E) YAF2–PDCD5–TP53 signaling network mediates genotoxic stress response. Cells were transfected with the indicated set of PDCD5 point mutants. Cell viability was assessed by the MTT assay (upper & left panel). The results are shown as means ± SD calculated from four independent experiments. *, $P < 0.05$. Whole cell lysates were analyzed by western blotting with the indicated antibodies (upper & right panel). Fixed cells were immunostained with r-H2AX antibody (lower panel). Representative blots and images of four independent experiments are shown. Bar scale = 10 μm. (F) Impaired YAF2–PDCD5–TP53 signaling network confers the chemoresistance of A549 cells. The cells were injected subcutaneously into the right flank of nude mice. Four weeks after injection, mice with comparable-sized tumors (~200 mm^3) were selected for treatment with ET (10 mg/kg) at 2-day interval for seven weeks. Tumor volumes were measured every week. *, $P < 0.05$ vs. without ET; #, $P < 0.05$ vs. with ET; **, $P < 0.05$ vs. with ET + shPDCD5. Error bars indicate SD ($n = 6$ per group). (G) Model of our findings. Genotoxic stress triggers the association of YAF2 and PDCD5 for PDCD5 stabilization via inhibiting the ubiquitination of PDCD5. This association subsequently leads to TP53 stabilization and activation of genotoxic stress response.

[37] J.L. Kalenik, D. Chen, M.E. Bradley, S.J. Chen, T.C. Lee, Yeast two-hybrid cloning of a novel zinc finger protein that interacts with the multifunctional transcription factor YY1, Nucleic Acids Res. 25 (1997) 843–849.
[38] D. Bannasch, B. Madge, M. Schwab, Functional interaction of Yaf2 with the central region of MycN, Oncogene 20 (2001) 5913–5919.
[39] S.E. Stanton, L.J. McReynolds, T. Evans, N. Schreiber-Agus, Yaf2 inhibits caspase 8-mediated apoptosis and regulates cell survival during zebrafish embryogenesis, J. Biol. Chem. 281 (2006) 28782–28793.
[40] Z. Gao, J. Zhang, R. Bonasio, F. Strino, A. Sawai, F. Parisi, Y. Kluger, D. Reinberg, PCGF homologs, CBX proteins, and RYBP define functionally distinct PRC1 family complexes, Mol. Cell 45 (2012) 344–356.
[41] L.A. Carvajal, J.J. Manfredi, Another fork in the road—life or death decisions by the tumour suppressor p53, EMBO Rep. 14 (2013) 414–421.